ACS OMEGA

Open Access

http://pubs.acs.org/journal/acsodf

Article

PEGylated Chitosan Nanoparticles Loaded with Betaine and Nedaplatin Hamper Breast Cancer: In Vitro and In Vivo Studies

Sherif Ashraf Fahmy,[¶] Asmaa Ramzy,[¶] Nourhan M. El Samaloty,[¶] Nada K. Sedky, and Hassan Mohamed El-Said Azzazy*

Cite This: *ACS Omega* 2023, 8, 41485−41494

Read Online

ACCESS | Metrics & More | Article Recommendations | Supporting Information

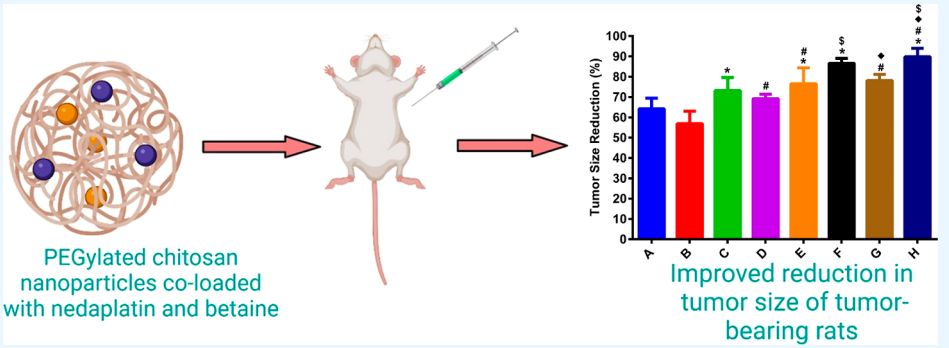

ABSTRACT: The current study investigates the anticancer effects of PEGylated chitosan nanoparticles (CS NPs) coloaded with betaine (BT) and nedaplatin (ND) on breast adenocarcinoma (MCF-7) cells and breast cancer-bearing rats. Hereof, the ionotropic gelation approach was implemented for the synthesis of PEG-uncoated and PEG-coated CS NPs encompassing either BT, ND, or both (BT-ND). The sizes of the developed BT/CS NPs, ND/CS NPs, and BT-ND/CS NPs were 176.84 ± 7.45, 204.1 ± 13.6, and 201.1 ± 23.35 nm, respectively. Meanwhile, the sizes of the synthesized BT/PEG-CS NPs, ND/PEG-CS NPs, and BT-ND/PEG-CS NPs were 165.1 ± 32.40, 148.2 ± 20.98, and 143.7 ± 7.72 nm, respectively. The surface charges of the fabricated nanoparticles were considerably high. All of the synthesized nanoparticles displayed a spherical form and significant entrapment efficiency. Release experiments demonstrated that the PEGylated and non-PEGylated CS NPs could discharge their contents into the tumor cells' microenvironments (pH 5.5). In addition, the NPs demonstrated an outstanding ability to reduce the viability of the MCF-7 cell line. In addition, BT-ND/PEG-CS NPs were found to be the strongest among all NP preparations, where they caused around 90% decrease in the size of mammary gland tumors in rats compared to vehicle-treated animals.

1. INTRODUCTION

Cancer is still one of the foremost reasons for global mortality.[1] With an anticipated 2.3 million new cases (12.5% of all cancers), female breast cancer has transcended lung cancer as the most commonly diagnosed malignancy.[1] Breast cancer (BC) is the most prevalent malignancies among women, accounting for more than one out of every ten newly diagnosed cancer cases yearly.[2] Radiation, chemotherapeutics, and surgical interventions are considered to be the mainstay of treatment for most BC patients. Despite considerable advancements in early detection methods, surgical methodologies, and novel therapeutic modalities such as molecular targeting and immunotherapeutic approaches, the incidence of BC is still alarmingly rising. Therefore, nanoformulation of chemotherapeutics could improve their physicochemical properties and reduce their systematic side effects.[3] Additionally, investigating the molecular mechanisms involved in BC's malignant transformation and metastasis would shed light on key molecules that could be targeted for its prevention.[4−7]

Platinum-based chemotherapies are still the standard first-line chemotherapy regimen for many solid tumors, including BC.[8−11] Nedaplatin is a cisplatin analogue that has been approved in Japan for cancer treatment.[12,13] Compared to cisplatin, nedaplatin exerts less toxic side effects, namely, nephrotoxicity and gastrointestinal toxicity, and overcomes cisplatin resistance. The nedaplatin-based chemotherapeutic regimen was well tolerated and effectively enhanced the quality of life of BC patients.[14,15] However, nedaplatin (ND) resistance and its substantial toxic reactions considerably hamper its worldwide acceptance.[16] Attempts to overcome the drawbacks of nedaplatin and other platinum-based chemotherapeutics

Received: July 24, 2023
Accepted: October 6, 2023
Published: October 25, 2023

include nanoformulation into different nanocarriers to enhance their selective internalization into cancer cells while simultaneously reducing their off-target side effects and their elimination from systemic circulation.[17] In this regard, the enhanced permeability and retention (EPR) effect, caused by the permeable vascular system and inadequate lymphatic drainage within tumors, is leveraged to drive nanoparticles to target tumor cells successfully.[18]

Many nanosystems, including polymeric nanoparticles, have been developed for the controlled release of various natural and synthetic drugs.[19] Chitosan, a natural polysaccharide, has been extensively investigated for the delivery of different drugs. Chitosan has major advantages, including biodegradability and biocompatibility.[20−22] In addition to their use as drug delivery vehicles for various synthetic and natural chemicals, chitosan nanoparticles (CS NPs) have antioxidant, anticancer, and antibacterial effects.[23] Recently, chitosan was used as an adjuvant vaccine with the potential to modulate the tumor microenvironment (TME) in several malignant contexts.[24] Encapsulation of drugs into CS NPs improves their biodistribution and reduces their side effects.[25] PEG-modified CS NPs are considered promising nanosystems for potent anticancer delivery mainly because PEG decreases NP recognition by the reticuloendothelial system (RES), thereby extending their circulation period.[26]

Betaine (BT), also known as trimethyl glycine, is a stable, natural, and nontoxic methyl donor that supports DNA methylation (at doses up to 15 g per day).[27] Shrimps, wheat germ, and sugar beets are examples of reliable sources of BT.[28] BT can act as an antitumor agent by inhibiting angiogenesis by forming complex coacervates.[29]

Despite the tremendous efforts made by researchers and clinicians to provide personalized, tailored therapeutic options for different molecular subtypes of BC patients, therapeutic outcomes are still inadequate. Chitosan, a functional biopolymer, has been used in multiple formulas to deliver chemotherapeutics owing to its anticancer activities, immunomodulatory properties, biocompatibility, and biodegradability. The ionotropic gelation method was used to generate PEG-uncoated and PEG-coated CS NPs (CS) loaded with BT, ND, or a combination of BT and ND. The prepared nanoparticles' average size and shape, surface charge, and entrapment efficiency were studied. In addition, Fourier transform infrared spectroscopy (FTIR) was used to verify the chemical structure of the designed nanoparticles. Furthermore, the release profiles of BT, ND, and BT-ND from poly(ethylene glycol) (PEG)-uncoated and PEG-coated Cs NPs were assessed at acidic and physiological pH. The cytotoxicity of the fabricated nanoparticles against MCF-7 cells was evaluated and compared to free BT and ND. The possibility of BT augmenting nedaplatin when both compounds are coloaded in PEG-uncoated/PEG-coated CS NPs was studied. The anticancer effects of the nanoformulations were also examined in the BC-bearing rat model.

2. MATERIALS AND METHODS

2.1. Animals. All animal experiments were performed using 60 female Wistar rats at the animal house of the National Research Center (Cairo, Egypt). All animal experiments were carried out following the rules and regulations of the EU Directive 2010/63/EU for animal experiments. The experimental work received approval (REC-EPSPI-9/59) from the Research Ethics Committee at the Faculty of Pharmacy, Future University in Egypt. Food and water were adjusted and offered to rats by the staff members. Rats were left for 7 days to become accustomed to environmental changes before the beginning of the experiments. Polypropylene cages were utilized as shelters for the animals. Each cage accommodated two rats. Random segregation of rats into the control or various treated groups was performed. Animals were kept at 22 ± 2 °C and exposed to 12 h cycles of light and darkness.

Table 1. Animal Groups

group I	control (negative control)
group II	DMBA-induced rats only (positive control for induction of BC)[34]
group III	following tumor development, DMBA-induced rats were injected with 15 mg/kg/week ND for 6 weeks[35]
group IV	following tumor development, DMBA-induced rats were injected with 15 mg/kg/week BT for 6 weeks
group V	following tumor development, DMBA-induced rats were injected with 15 mg/kg/week ND/CS NPs for 6 weeks
group VI	following tumor development, DMBA-induced rats were injected with 15 mg/kg/week BT/CS NPs for 6 weeks
group VII	following tumor development, DMBA-induced rats were injected with 15 mg/kg/week BT-ND/CS NPs for 6 weeks
group VIII	following tumor development, DMBA-induced rats were injected with 15 mg/kg/week ND/PEG-CS NPs for 6 weeks
group IX	following tumor development, DMBA-induced rats were injected with 15 mg/kg/week BT/PEG-CS NPs for 6 weeks
group X	following tumor development, DMBA-induced rats were injected with 15 mg/kg/week BT-ND/PEG-CS NPs for 6 weeks

2.2. Materials. Nedaplatin, betaine, PEG 400, and DMBA (7,12-dimethylbenz[*a*]anthracene) were acquired from Sigma-Aldrich, St. Louis, MO. Low-molecular-weight chitosan was obtained from Biosynth, Carbosynth (Berkshire, UK). Sodium tripolyphosphate (TPP) was obtained from Advent (Mumbai, India). Both Dulbecco's modified Eagle's medium (DMEM) supplemented with 4.5 g/L glucose and Trypan Blue were provided by Lonza Bioscience (Walkersville, MD). Trypsin, phosphate-buffered saline (PBS, pH 7.4), DMEM, and dimethyl sulfoxide (DMSO) were purchased from Serva (Heidelberg, Germany). Ethanol and 3-(4,5-dimethylthiazol-2-yl)-2,5-diphenyltetrazolium bromide (MTT) were purchased from Thermo Fisher Scientific (Waltham, MA). Fetal bovine serum (FBS) was obtained from Gibco (Waltham, MA). MCF-7 cells were purchased from ATCC (Manassas, VA).

2.3. Methods. *2.3.1. Synthesis of the CS NPs.* CS NPs loaded with BT, ND, and BT-ND were prepared using the ionotropic gelation method, as described elsewhere, with few alterations.[30,31] In brief, 1 mg mL^{-1} chitosan solution was prepared using 2% (v/v) glacial acetic acid. The pH of the solution was kept at 4 through the utilization of 10 M NaOH. The aqueous solution was filtered (0.45 μm syringe filters) and magnetically stirred (24 h). Then, 200 μL of TPP (1 mg mL^{-1}), as a cross-linker, was blended with BT, ND, or BT-ND and added dropwise to CS solution (5 mL) while stirring. This resulted in BT/CS NPs, ND/CS NPs, and BT-ND/CS NPs.

PEG-coated CS NPs loaded with BT, ND, and BT-ND were produced by the dropwise addition of 250 μL of PEG 400 to a chitosan solution (5 mL) and stirring for 30 min. The cross-linker TPP (1 mg mL^{-1}) was then combined with BT, ND, or BT-ND, which were then added to PEG CS solution. This resulted in the formation of BT/PEG-CS NPs, ND/PEG-CS NPs, and BT-ND/PEG-CS NPs.

2.3.2. Characterization of the Designed CS NPs. The average size, PDI, and surface charge of different nano-

https://doi.org/10.1021/acsomega.3c05359
ACS Omega 2023, 8, 41485−41494

Table 2. Characterization and EE % of the Different PEG-Uncoated Chitosan Nanoparticles[a]

nanoparticles	size (nm)	PDI	zeta-potential (mV)	EE (%)	
				BT	ND
CS NPs	290.3 ± 7.5	0.21 ± 0.01	+27.6 ± 1.5		
BT/CS NPs	176.8 ± 8.9	0.26 ± 0.04	+31.9 ± 9.3	71.2 ± 1.9	
ND/CS NPs	204.1 ± 13.6	0.27 ± 0.05	+41.4 ± 2.4		73.5 ± 2.3
BT-ND/CS NPs	201.1 ± 23.4	0.31 ± 0.04	+38.9 ± 2.3	70.4 ± 3.1	72.1 ± 2.4

[a]Results are means of three independent experiments ± SD.

Table 3. Characterization and EE % of the Different PEG-Coated Chitosan Nanoparticles[a]

nanoparticles	size (nm)	PDI	zeta-potential (mV)	EE (%)	
				BT	ND
PEG-CS NPs	273.3 ± 2.7	0.29 ± 0.07	+15.7 ± 1.0		
BT/PEG-CS NPs	165.1 ± 32.4	0.28 ± 0.07	+20.5 ± 2.1	88.7 ± 2.4	
ND/PEG-CS NPs	148.2 ± 21	0.32 ± 0.06	+9.47 ± 2.1		90.2 ± 1.9
BT-ND/PEG-CS NPs	143.7 ± 7.7	0.28 ± 0.05	+24.7 ± 2.2	89.4 ± 2.9	91.6 ± 2.8

[a]Results are means of three independent ± SD.

formulations were studied using a zeta sizer Nano ZS (Malvern Instruments, Herrenberg, Germany), at 25 °C. Transmission electron microscopy (JEOL-JEM 2100, Musashino, Tokyo, Japan) was used to study the morphology of the synthesized NPs.

The chemical features of the NPs were studied by using FTIR spectroscopy (Shimadzu, Kyoto, Japan).

2.3.3. Entrapment Efficiency (EE %). The EE % of BT/CS NPs, ND/CS NPs, BT-ND/CS NPs, BT/PEG-CS NPs, ND/PEG-CS NPs, and BT-ND/PEG-CS NPs was determined as previously detailed with minor changes.[32] In brief, each sample (2 mL) was centrifuged (15,000 rpm) for 2 h at 4 °C (Hermle Z326 K, Labortechnik GmbH, Wehingen, Germany). Free BT, ND, and BT-ND in the formulation supernatant were then quantified using HPLC (Supporting Information). Equation 1 was used to determine the EE % of the prepared nanoformulations.[33]

$$\text{EE (\%)} = \frac{\text{total drug amount} - \text{drug amount in supernatant}}{\text{total drug amount}} \times 100 \quad (1)$$

The DLC % was determined using eq 2.

$$\text{DLC \%} = \frac{\text{amount of loaded drug}}{\text{initial amount of drug} + \text{initial amount of polymer}} \times 100 \quad (2)$$

2.3.4. Release Study. In order to study the release rates of BT and ND from different CS NP formulas, the dialysis bag approach was investigated at physiological and cancerous cell pH (7.4 and 5.5, respectively). Concisely, each formula (0.5 mL) was dialyzed in 25 mL of PBS (of two different pH values) and then incubated in a shaking incubator, rotating at 150 rpm at 37 °C. At certain time points, a specific amount of each sample was drawn and instantly substituted with fresh PBS (1 mL).

2.3.5. Cytotoxicity. MCF-7 cells were cultured in 96-well plates under the standard conditions. Basically, cells were maintained in culture plates containing DMEM, 5% penicillin−streptomycin, and FBS (10%). The culture plates were situated in a 5% CO_2 incubator with the temperature adjusted to 37 °C. A hemocytometer was used to count viable cells after being stained with Trypan blue. About 10,000 MCF-7 cells were added in each well for 24 h before being treated for another 48 h with increasing doses of free or nanoformulated drugs. The supernatant was decanted upon cessation of treatment, and 20 μL of MTT solution (5 mg/mL) was mixed with 80 μL of medium for 3 h. The supernatant was decanted and substituted with 100 μL of DMSO. The plates were read at 570 nm. The vitality of MCF-7 cells was detected using the formula

$$A(\text{sample})/A(\text{control}) \times 100$$

MCF-7 cells grown in a serum-free medium treated with vehicle (CS or PEG CS NPs) served as the control.

2.3.6. BC Rat Model. 2.3.6.1. Experimental Protocol. Female Wistar rats (55−60 days; 180−200 g) were classified into 10 groups of 6 animals each, as shown in Table 1.

After dosing, the rats were anesthetized with diethyl ether and sacrificed in the diestrus phase of the estrous cycle. Blood was collected, and the serum was separated for assays of molecular biomarkers.

2.3.6.2. Tumor Size Reduction (%). Mammary gland tumors were induced in female Wistar rats (55 days, 180−200 g) by intravenous injection of a freshly prepared single dose of 20 mg/mL DMBA diluted in corn oil. By the 13th week, tumors appeared in all rats. Guided by the former study of Matsumoto et al.[36] and the calculated IC_{50}s in this study, all investigated agents (ND, BT, ND/CS NPs, BT/CS NPs, BT-ND/CS NPs, ND/PEG-CS NPs, BT/PEG-CS NPs, and ND-BT/PEG-CS NPs) were delivered to the rats at a volume of 0.1 mL/10 g body weight. At the end of the treatment period, rats in all groups were sacrificed using thiopental (IP 200 mg/kg). Tumor volume and body weight were recorded after the induction at 3 weeks of treatment and after 6 weeks of treatment.[37] The tumor size reduction % was computed using eq 3.

$$\text{EE (\%)} = \frac{\text{initial tumor size} - \text{final tumor size}}{\text{initial tumor size}} \times 100 \quad (3)$$

2.3.7. Statistical Analysis. Ordinary one-way analysis of variance (ANOVA) was used, followed by the Tukey HSD multiple comparisons test to compare different groups. *P* values < 0.05 were considered significant. All statistical analyses were

https://doi.org/10.1021/acsomega.3c05359
ACS Omega 2023, 8, 41485−41494

performed using SPSS Statistics v. Twenty for Windows (SPSS, Chicago, IL). The graphs were plotted using GraphPad Prism 7. All results were reported as the mean of three measurements ± SD.

3. RESULTS AND DISCUSSION

3.1. Characterization of PEGylated and Non-PEGylated CS NPs. Dynamic light scattering was involved in studying the average sizes and PDI of PEG-uncoated and PEG-coated chitosan NPs, and the results are summarized in Tables 3 and 4. All prepared nanoparticles had diameters between 140 and 295 nm, which were previously described for various nanoparticles encompassing antitumor agents. This size range allows NPs and their payload of drugs to accumulate passively in cancer cells with loose vascularity and deprived lymphatic drainage.[38,39] As shown in Table 2, the surface charges of the synthesized nanoparticles were highly cationic (+27.60 ± 1.48, +31.91 ± 9.27, +41.4 ± 2.36, and +38.975 ± 2.28 mV for CS NPs, BT/CS NPs, ND/CS NPs, and BT-ND/CS NPs, respectively) and originated from chitosan. These high surface charges would impart high stability to the designed NPs. The DLC % of BT and ND in BT/CS NPs and ND/CS NPs were 8.14 and 9.44%, respectively. While the DLC % of BT and ND in BT-ND/CS NPs were 6.91 and 7.84%, respectively. In addition, Table 2 shows the synthesized CS nanoparticles' entrapment efficiencies, demonstrating CS NPs to carry high percentages of either BT, ND, or BT and ND.

Modifying the surface of CS NPs via PEGylation was reported to improve their physicochemical and biological properties.[40,41]

The PDI and size were reduced by coating CS NPs with PEG (Table 3). This is because, during the cross-linking process, PEG forms an interpenetrating structural network with chitosan, enhancing the compactness and uniformity of the NPs' surface, thus decreasing their diameter and surface charges following PEGylation.[42] Additionally, the surface charge of PEG-coated CS NPs has decreased, as compared to the uncoated CS NPs, owing to shielding the chitosan cationic amine groups by the anionic PEG chains.[42] The DLC % of BT and ND in BT/PEG-CS NPs and ND/PEG-CS NPs were 10.32 and 11.17,

Table 4. IC_{50} Values of Blank CS NPs, PEG-Coated CS NPs, Pure Betaine, Pure Nedaplatin, Unmodified CS NPs, BT/CS NPs, ND/CS NPs, BT-ND/CS NPs, PEG-CS NPs, BT/PEG-CS NPs, ND/PEG-CS NPs, and BT-ND/PEG-CS NPs[a]

treatment	IC_{50} (μg/mL)
CS NPs	>300
PEG-CS NPs	>300
BT	121.85 ± 13.6
ND	50.82 ± 9.8
BT/CS NPs	#79.32 ± 8.1
ND/CS NPs	*21.7 ± 7.8
BT-ND/CS NPs	#*4.78 ± 2.1
BT/PEG-CS NPs	#73.95 ± 3.7
ND/PEG-CS NPs	a*7.94 ± 1.9
BT-ND/PEG-CS NPs	#*♦a2.77 ± 0.7

[a]The treatment period was 48 h. IC_{50} values are presented as the mean of triplicate runs ± standard deviation (SD). The symbol (#) refers to the statistical significance of the BT-treated cells. The symbol (*) refers to the statistical significance ($p < 0.05$) of the ND-treated cells. The symbols (♦) and (a) refer to statistical significance from BT/CS NPs and ND/CS NPs, respectively.

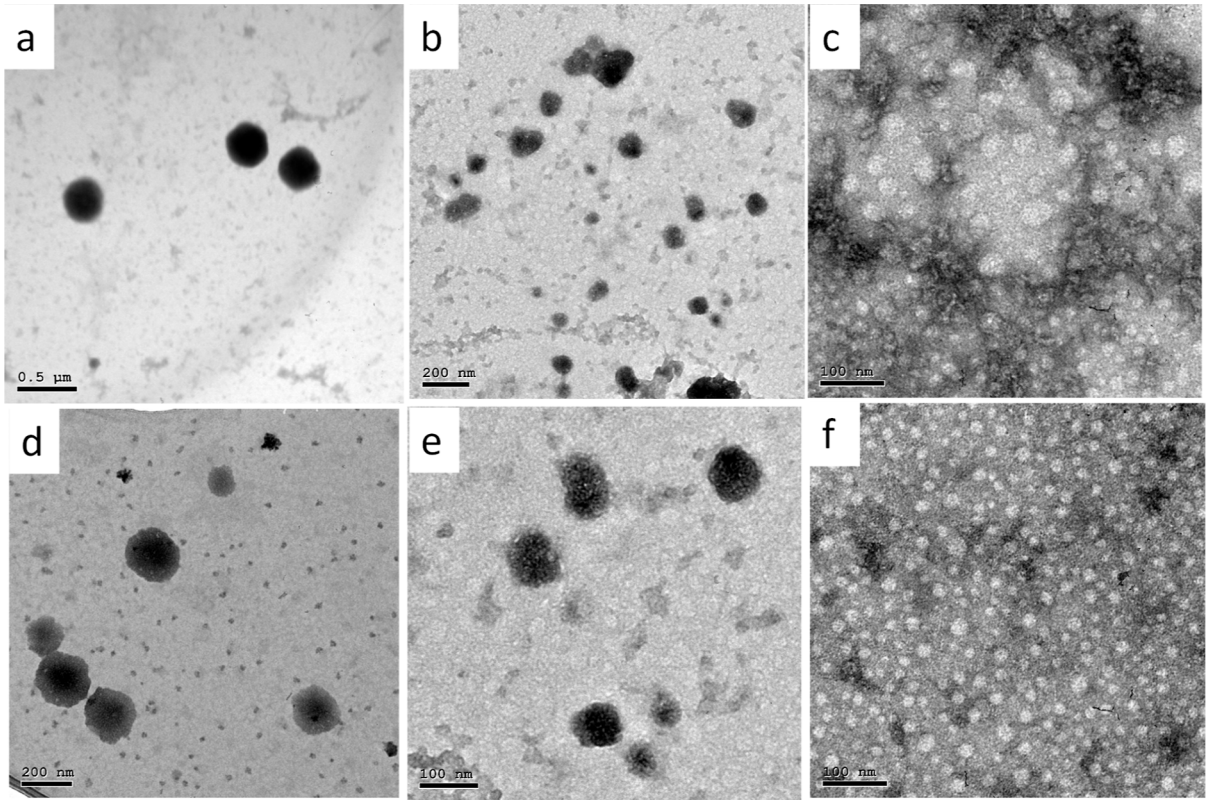

Figure 1. TEM images of (a) BT/CS NPs, (b) ND/CS NPs, (c) BT-ND/CS NPs, (d) BT/PEG-CS NPs, (e) ND/PEG-CS NPs, and (f) BT-ND/PEG-CS NPs.

https://doi.org/10.1021/acsomega.3c05359
ACS Omega 2023, 8, 41485−41494

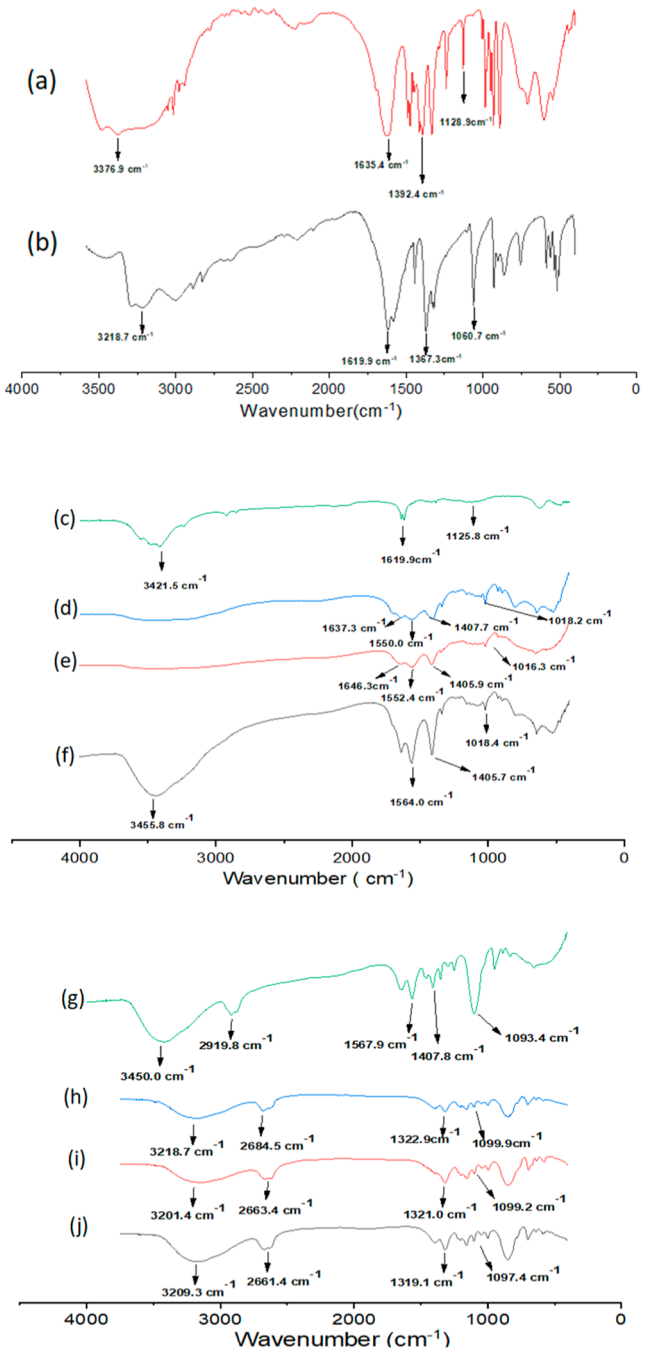

Figure 2. FTIR spectra of (a) free BT, (b) free nedaplatin, (c) PEG-uncoated CS NPs, (d) BT/CS NPs, (e) ND/CS NPs, (f) BT-ND/CS NPs, (g) PEG-CS NPs, (h) BT/PEG-CS NPs, (i) ND/PEG-CS NPs, and (j) BT-ND/PEG-CS NPs.

respectively. While DLC % of BT and ND in BT-ND/PEG-CS NPs were 9.21 and 10.54%. Our findings showed that PEGylation of chitosan NPs (loaded with BT, ND, or BT-ND) has improved the DLC % and EE % of either BT or ND owing to the colloidal stabilization impact of PEG chains on the CS NP exteriors.[31] ND/CS NPs and BT-ND/CS NPs were successfully formed with spherical shapes and smooth surfaces. TEM analysis also revealed that modifying the CS NPs surface with PEG had no impact on their globular morphologies (Figure 1).

3.2. Fourier-Transform Infrared Spectroscopy. The FTIR spectrum of BT exhibited four major peaks at 3376.9 cm^{-1} (−OH stretching), 1635.4 cm^{-1} (C═O stretching), 1392.4 cm^{-1} (−CH bending), and 1128.9 cm^{-1} (C−O−C) (Figure 2a).[43] In addition, the spectrum of ND revealed four distinct peaks at 3218.7 cm^{-1} (−OH stretching), 1619.9 cm^{-1} (C═C), 1367.3, and 1060.7 cm^{-1} (C═C) (Figure 2b).[44,45]

The stretching vibrations of amine ($-NH_2$) and/or hydroxyl (−OH) and (C═C bond) and carboxylic (C═O bond) groups may correspond to distinct peaks in the FTIR spectra of CS NPs at 3420 and 1620 cm^{-1}, respectively. A peak at 1126 cm^{-1} was also identified, equivalent to an alcoholic (C−O) stretching vibration[46] (Figure 2c). The FTIR spectra of BT/CS NPs, ND/CS NPs, and BT-ND/CS NPs (Figure 2d−f), on the other hand, displayed all main peaks of BT, ND, and CS NPs with no notable shifts, indicating physical incorporation of BT and ND within the CS matrix.[47] Furthermore, a single peak was identified at 2919.8 cm^{-1}, which could be ascribed to the ($-CH_2$) stretching vibration. This shows that the CS NPs were successfully coated with PEG (Figure 2g). All major BT, ND, and PEGylated CS NPs peaks were verified in the spectra of BT/PEG-CS NPs, ND/PEG-CS NPs, and BT-ND/PEG-CS NPs (Figure 2h−j), indicating the physical entrapment of ND and BT within the CS matrix. These findings are consistent with previous reports that described the synthesis of PEGylated nanocarriers.[48]

3.3. Release Study. The release of BT and ND from the CS NPs was investigated at pH 7.4 and pH 5.5 (tumor cells' microenvironment). The released BT and ND were quantified using HPLC (Supporting Information). The CS and PEG-coated CS NPs were stable at pH 7.4. Regarding CS NPs (Figure 3), around 28.9 and 29.7% of the entrapped BT and ND were eluted after 72 h from BT/CS NPs and ND/CS NPs, respectively. In addition, 32.9 and 33.8% of the entrapped BT and ND were discharged from BT-ND/CS NPs, at 37 °C, after 72 h. Concerning the PEG-coated CS NPs (Figure 4), 33.8 and 31.1% of the entrapped BT and ND were eluted after 72 h from BT/PEG-CS NPs and ND/PEG-CS NPs, respectively. At the same time, 30.5 and 31.2% of the entrapped BT and ND, respectively, were released from BT-ND/PEG-CS NPs, at 37 °C, after 72 h.

On the other hand, both CS NPs and PEG-CS NPs displayed faster drug release percentages at acidic pH 5.5 in comparison to release at physiological pH. Regarding CS NPs, 71 and 73% of the entrapped BT and ND were effluxed after 72 h from BT/CS NPs and BT/CS NPs, respectively, at pH 5.5. At the same time, 75 and 76% of the entrapped BT and ND, respectively, were effluxed from BT-ND/CS NPs after 72 h. Regarding PEG-coated CS NPs, 88.3 and 89.7% of the entrapped BT and ND were released after 72 h from BT/PEG-CS NPs and ND/PEG-CS NPs, respectively. At the same time, 92.5 and 94.6% of the entrapped BT and ND, respectively, were released after 72 h from BT-ND/PEG-CS NPs. These findings revealed that the PEG layer around the CS NPs has increased the release of drugs at pH 5.5. In the acidic microenvironment, the chitosan amino groups are protonated, enhancing the disassembling of the cross-linked chitosan chains and allowing the penetration of the CS NPs by the release medium. Consequently, this leads to the faster release of BT and ND from the nanoparticles.[30] The increased release of BT and ND in the acidic tumor microenvironment would ultimately enhance the selective targeting of the entrapped drugs to BC cells.

Moreover, the drugs were released from the polymeric matrix by desorption, erosion, degradation, and diffusion mecha-

https://doi.org/10.1021/acsomega.3c05359
ACS Omega 2023, 8, 41485−41494

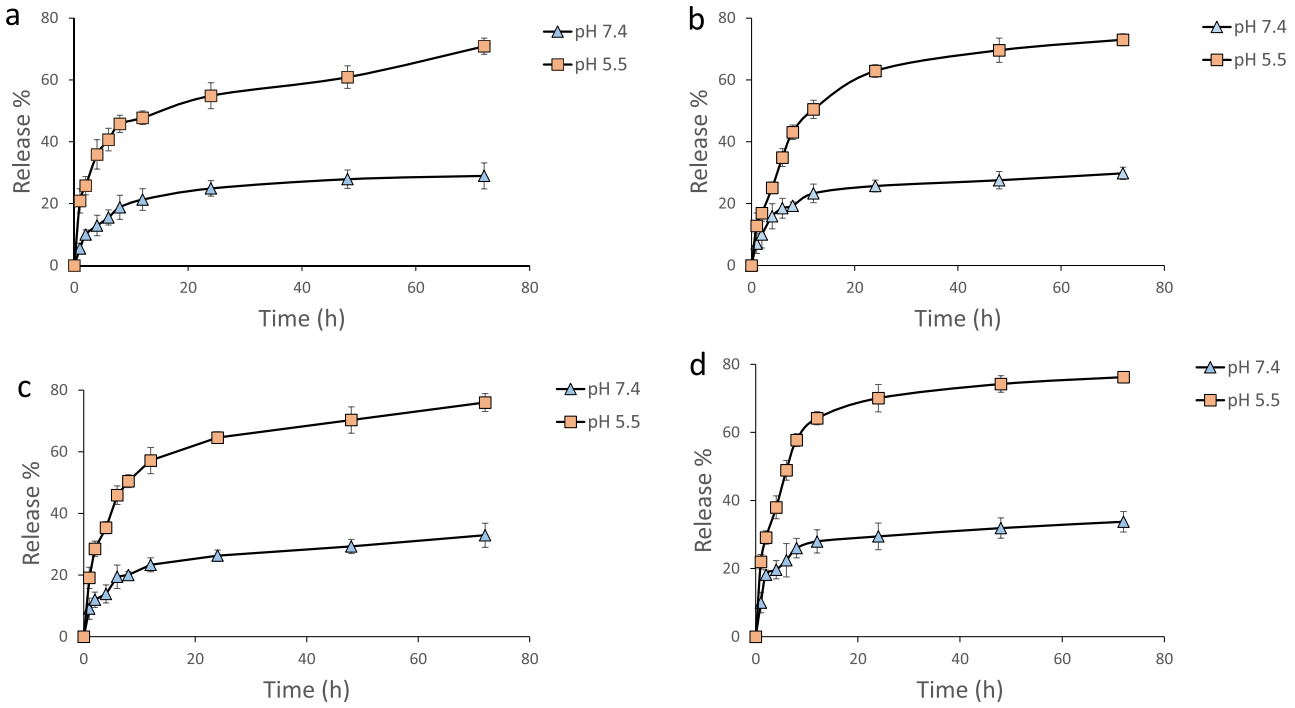

Figure 3. Release percentages of (a) BT from BT/CS NPs, (b) ND from ND/CS NPs, (c) BT from BT-ND/CS NPs, and (d) ND from BT-ND/CS NPs at two different pH values.

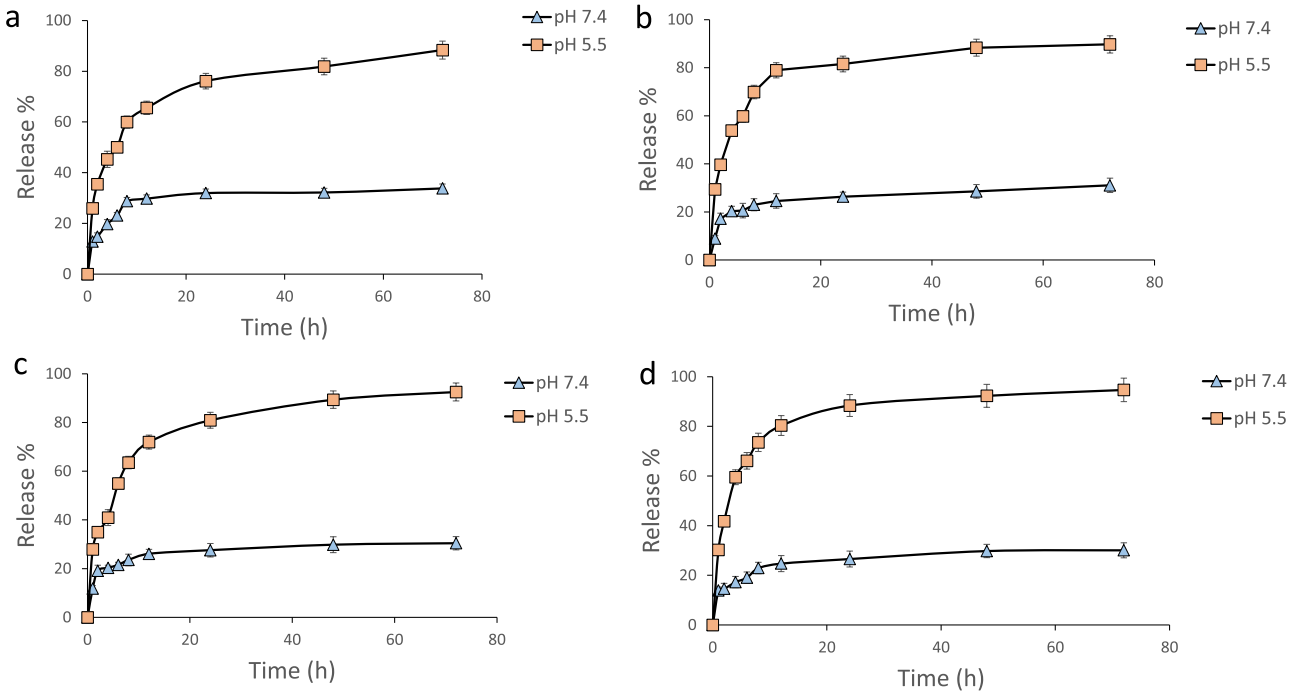

Figure 4. Release percentages of (a) BT from BT/PEG-CS NPs, (b) ND from ND/PEG-CS NPs, (c) BT from BT-ND/PEG-CS NPs, and (d) ND from BT-ND/PEG-CS NPs at 37 °C at two different pH values.

nisms.[49] The burst release observed in our study might be attributed to the amount of payload scattered on the polymer's surface.[50] After 72 h, approximately 70−89% of the loaded drugs were released from uncoated and coated CS NPs. These results align very well with previous studies conducted by Meng et al.,[51] Ulu et al.,[52] and Zhang et al.,[53] who reported the release of 50−70, 80−90, and 80% of the loaded drugs from CS NPs within 48−72 h, respectively. Thus, our findings agree very well with those of the previous reports. In addition, grafting with hydrophilic, biodegradable, and biocompatible PEG polymers improves the solubility in water.[54] PEG serves as a cross-linker that facilitates drug release via increasing hydrophilicity and through its swelling capability, which eventually increases the drug release.[55]

3.4. Cytotoxicity. MTT assay was conducted on MCF-7 cells treated with ten increasing concentrations (ranging from

https://doi.org/10.1021/acsomega.3c05359
ACS Omega 2023, 8, 41485−41494

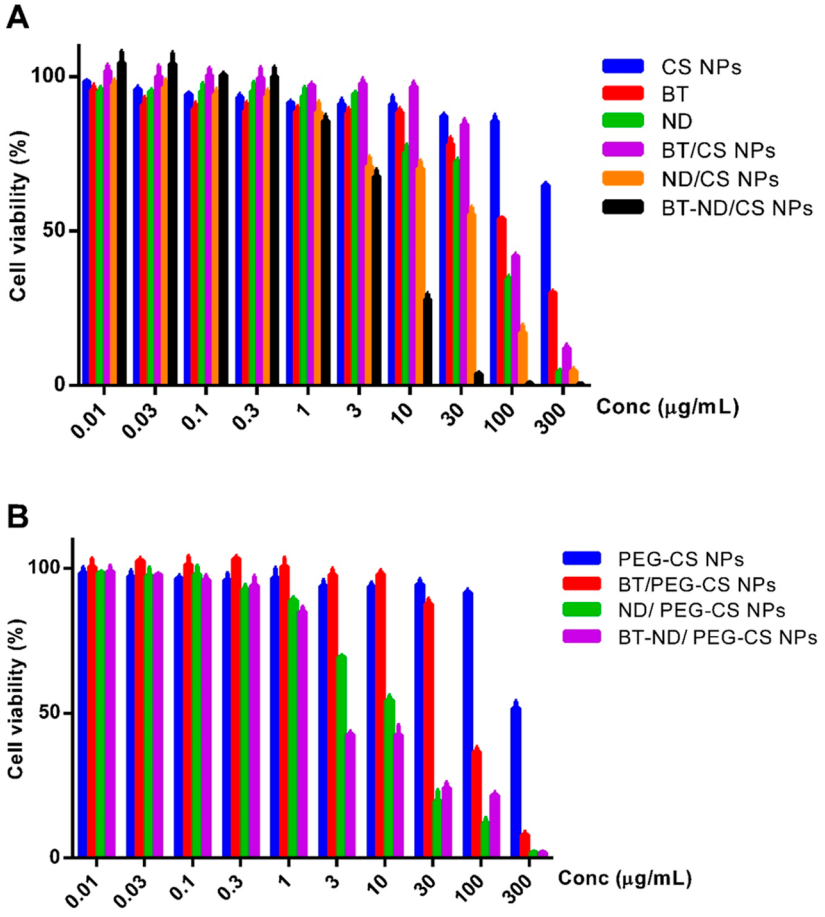

Figure 5. Cell viability of MCF-7 cells after treatment with both (A) non-PEGylated and (B) PEGylated chitosan particles for 48 h. The values are presented as the mean ± the standard deviation (SD) of three independent trials.

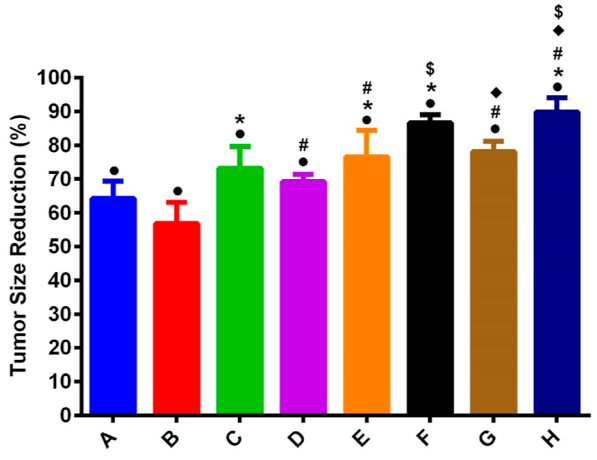

Figure 6. Tumor size reduction % in rats that received treatment with (A) ND, (B) BT, (C) ND/CS NPs, (D) BT/CS NPs, (E) BT-ND/CS NPs, (F) ND/PEG-CS NPs, (G) BT/PEG-CS NPs, and (H) ND-BT/PEG-CS NPs as compared to the DMBA-only group. The results are displayed as the mean of triplicate experiments ± the standard deviation (SD). The symbols (●), (#), and (*) refer to statistical significance from DMBA-only group, BT-treated cells, and ND-treated cells, respectively. The symbols (♦) and ($) refer to statistical significance from BT/CS NPs and ND/CS NPs, respectively. *P*-value ≤ 0.05 is considered statistically significant.

0.01 to 300 μg/mL) of free BT, free nedaplatin, BT/CS NPs, ND/CS NPs, BT-ND/CS NPs, PEG-CS NPs, BT/PEG-CS NPs, ND/PEG-CS NPs, and BT-ND/PEG-CS NPs, in addition to blank CS NPs and PEG-coated CS NPs, for 48 h. The percentage of viable cells was drawn against the different concentrations of both non-PEGylated and PEGylated CS nanoparticles (Figure 5), and IC_{50} values were calculated (Table 4) and used for further investigations. Former studies have shed light on the importance of encapsulating platinum-based anticancer agents to minimize systemic toxicity, enhance the retention of the administered drugs at the tumor site, and avoid their degradation.[56] In this study, the synthesized CS nanoparticles (BT/CS NPs and ND/CS NPs) showed a remarkable increase in the cytotoxic activity against MCF-7 compared to their corresponding free drugs, BT and ND. These results support a previously published report where the encapsulation of ND into cucurbiturils host molecules improved the antitumor activity against MCF-7 more than the free drug.[57] Moreover, in the current study, the PEGylated CS nanoparticles even displayed a cytotoxic activity against MCF-7 higher than that of the non-PEGylated CS nanoparticles. Likewise, a former study suggested that oxaliplatin encapsulated in PEG-CS NPs displayed a lower IC_{50} (17.98 ± 3.99 μg/mL), i.e., higher antitumor activity against MCF-7 cells than the oxaliplatin encapsulated in non-PEGylated CS NPs with an IC_{50} of (23.88 ± 6.29 μg/mL).[30]

The current study included two nanoformulations for the combined BT and ND drug therapy, which, as speculated, showed the lowest IC_{50}s and were found to be the most potent formulations. The BT-ND/PEG-CS NPs displayed the lowest

https://doi.org/10.1021/acsomega.3c05359
ACS Omega 2023, 8, 41485−41494

IC_{50} (2.77 ± 0.7 μg/mL) among all of the investigated samples. This could be attributed to the synergistic effect of both BT and ND drugs and improved drug properties when they are encapsulated in PEGylated CS NPs.

3.5. In Vivo Studies in BC-Bearing Rat Model. *3.5.1. Effect on Tumor Volume.* Tumor volume increased with time in the DMBA-treated group and in all treated groups with different treatment regimens.

As shown in Figure 6, there was a significant reduction in the tumor size % ($p < 0.001$) in the groups that received ND, BT, BT/CS NPs, ND/CS NPs, BT-ND/CS NPs, BT/PEG-CS NPs, ND/PEG-CS NPs, and BT-ND/PEG-CS NPs treatments compared to the group that received no treatment (induced with DMBA only). The current in vivo findings support the in vitro cytotoxicity results on the MCF-7 cell line, whereby the fabricated nanoparticles demonstrated a higher ability to decrease the tumor size than the free drugs. Furthermore, the PEGylated nanoparticles reduced the tumor size more than the non-PEGylated nanoparticles. PEG has been shown to lengthen the circulation time of NPs by masking the NPs from recognition by the mononuclear phagocytic system, hence protecting them from destruction and elimination. As such, the time that PEGylated nanoparticles remain intact in circulation is more than that of the non-PEGylated nanoparticles.[58] Moreover, the PEGylated CS NPs possess positively charged surfaces that were noticed to facilitate the internalization of chemotherapeutic drugs by cancer cells as described by Lu and colleagues, who reported a remarkable increase in Paclitaxel (PTX) chitosan-modified PLGA nanoparticle internalization by MDA-MB-231 cells as compared to the free PTX.[59] It is worth mentioning that PTX-encapsulated PLGA nanoparticles' cellular uptake and cytotoxicity in different cancer cell lines were significantly improved by the PEG and chitosan coating.[60] Therefore, the considerable reduction in the tumor size observed in this study upon exposure to PEGylated NPs could be due to the immune evasion of the PEGylated nanoparticles, their positive surface charges, and improved cellular uptake.

The PEGylated nanoparticles containing the combination of ND and BT (BT-ND/PEG-CS NPs) showed the highest effect, causing an ∼90% reduction in the tumor size. These findings provide evidence that the antitumor activities of ND and BT are enhanced upon encapsulation in CS NPs and that PEG-coating of these NPs increases their activity. Furthermore, the coloading of BT with ND in CS NPs or CS-PEG NPs results in synergistic and chemosensitizing anticancer effects. To the best of our knowledge, the cytotoxic effect induced by ND and amplified by BT and CS NPs on BC has not been reported. Thus, in the presented study, we explored the proposition that combining ND and BT can augment the cytotoxic activity of ND on BC (in vitro and in vivo) and, hence, might prolong the survival duration in BC patients. Our findings suggested a novel potential role for the CS NPs, CS-PEG NPs, and even a surplus activity for the combined BT-ND/PEG NPs in reducing the BC tumor size. Therefore, the fabricated NPs were capable of causing remarkable repression of BC and possibly reducing chemoresistance to drug therapy.

4. CONCLUSIONS

Ionic gelation was used to develop PEG-uncoated and PEG-coated chitosan NPs that incorporated BT and/or ND. The PEG-modified CS NPs had smaller particle sizes, PDI, and zeta potential but more EE %. All synthesized NPs could release their payload in the acidic cancer microenvironment (pH 5.5) while remaining stable at physiological pH. BT-ND/PEG-CS NPs exerted the highest cytotoxicity against MCF-7 cells and had the most significant repression of tumor size in BC-bearing rats. These data suggest that BT-ND/PEG-CS NPs could further be investigated as a promising therapeutic strategy for treating BC.

■ ASSOCIATED CONTENT

Supporting Information

The Supporting Information is available free of charge at https://pubs.acs.org/doi/10.1021/acsomega.3c05359.

Additional experimental details for the quantification of the drugs (PDF)

■ AUTHOR INFORMATION

Corresponding Author

Hassan Mohamed El-Said Azzazy − *Department of Chemistry, School of Sciences & Engineering, The American University in Cairo, New Cairo 11835, Egypt; Department of Nanobiophotonics, Leibniz Institute of Photonic Technology, Jena 07745, Germany;* orcid.org/0000-0003-2047-4222; Phone: +2 02 2615 2559; Email: hazzazy@aucegypt.edu

Authors

Sherif Ashraf Fahmy − *Department of Chemistry, School of Life and Medical Sciences, University of Hertfordshire Hosted by Global Academic Foundation, Cairo 11835, Egypt;* orcid.org/0000-0003-3056-8281

Asmaa Ramzy − *Department of Chemistry, School of Sciences & Engineering, The American University in Cairo, New Cairo 11835, Egypt*

Nourhan M. El Samaloty − *Biochemistry Department, Faculty of Pharmacy and Drug Technology, Egyptian Chinese University, Cairo 11786, Egypt; Pharmacology and Biochemistry Department, Faculty of Pharmaceutical Sciences and Pharmaceutical Industries, Future University in Egypt, Cairo 12311, Egypt*

Nada K. Sedky − *Department of Biochemistry, School of Life and Medical Sciences, University of Hertfordshire Hosted by Global Academic Foundation, Cairo 11835, Egypt*

Complete contact information is available at: https://pubs.acs.org/10.1021/acsomega.3c05359

Author Contributions

¶S.A.F, A.R., and N.M.E.S. contributed equally to this work.

Notes

The authors declare no competing financial interest.

■ ACKNOWLEDGMENTS

This work was funded by a grant from the American University in Cairo to Prof. Dr. H.M.E.-S.A.

■ REFERENCES

(1) Sung, H.; Ferlay, J.; Siegel, R. L.; Laversanne, M.; Soerjomataram, I.; Jemal, A.; Bray, F. Global cancer statistics 2020: GLOBOCAN estimates of incidence and mortality worldwide for 36 cancers in 185 countries. *Ca-Cancer J. Clin.* **2021**, *71* (3), 209−249.

(2) Mahvi, D. A.; Liu, R.; Grinstaff, M. W.; Colson, Y. L.; Raut, C. P. Local cancer recurrence: the realities, challenges, and opportunities for new therapies. *Ca-Cancer J. Clin.* **2018**, *68* (6), 488−505.

(3) Sedky, N. K.; Abdel-Kader, N. M.; Issa, M. Y.; Abdelhady, M. M.; Shamma, S. N.; Bakowsky, U.; Fahmy, S. A. Co-Delivery of Ylang Ylang Oil of Cananga odorata and Oxaliplatin Using Intelligent pH-Sensitive

Lipid-Based Nanovesicles for the Effective Treatment of Triple-Negative Breast Cancer. *Int. J. Mol. Sci.* **2023**, *24* (9), 8392.
(4) Oeffinger, K. C.; Fontham, E. T. H.; Etzioni, R.; Herzig, A.; Michaelson, J. S.; Shih, Y.-C. T.; Walter, L. C.; Church, T. R.; Flowers, C. R.; LaMonte, S. J.; et al. Breast Cancer Screening For Women At Average Risk. *JAMA* **2015**, *314* (15), 1599−1614.
(5) Carninci, P.; Kasukawa, T.; Katayama, S.; Gough, J.; Frith, M.; Maeda, N.; Oyama, R.; Ravasi, T.; Lenhard, B.; Wells, C.; et al. The transcriptional landscape of the mammalian genome. *Science* **2005**, *309* (5740), 1559−1563.
(6) Yang, F.; Xue, X.; Bi, J.; Zheng, L.; Zhi, K.; Gu, Y.; Fang, G. Long noncoding RNA CCAT1, which could be activated by c-Myc, promotes the progression of gastric carcinoma. *J. Cancer Res. Clin. Oncol.* **2013**, *139*, 437−445.
(7) Yuan, J.-h.; Yang, F.; Wang, F.; Ma, J.-z.; Guo, Y.-j.; Tao, Q.-f.; Liu, F.; Pan, W.; Wang, T.-t.; Zhou, C.-c.; et al. A long noncoding RNA activated by TGF-β promotes the invasion-metastasis cascade in hepatocellular carcinoma. *Cancer Cell* **2014**, *25* (5), 666−681.
(8) Fahmy, S. A.; Ponte, F.; Grande, G.; Fawzy, I. M.; Mandour, A. A.; Sicilia, E.; Azzazy, H. M. E.-S. Synthesis, characterization and host-guest complexation of asplatin: improved in vitro cytotoxicity and biocompatibility as compared to cisplatin. *Pharmaceuticals* **2022**, *15* (2), 259.
(9) Ritacco, I.; Al Assy, M.; Abd El-Rahman, M. K.; Fahmy, S. A.; Russo, N.; Shoeib, T.; Sicilia, E. Hydrolysis in acidic environment and degradation of satraplatin: a joint experimental and theoretical investigation. *Inorg. Chem.* **2017**, *56* (10), 6013−6026.
(10) Fahmy, S. A.; Ponte, F.; Sicilia, E.; El-Said Azzazy, H. M. Experimental and Computational Investigations of Carboplatin Supramolecular Complexes. *ACS Omega* **2020**, *5* (48), 31456−31466.
(11) Sedky, N. K.; Braoudaki, M.; Mahdy, N. K.; Amin, K.; Fawzy, I. M.; Efthimiadou, E. K.; Youness, R. A.; Fahmy, S. A. Box-Behnken design of thermo-responsive nano-liposomes loaded with a platinum (iv) anticancer complex: evaluation of cytotoxicity and apoptotic pathways in triple negative breast cancer cells. *Nanoscale Adv.* **2023**, *5*, 5399−5413.
(12) Fahmy, S. A.; Preis, E.; Dayyih, A. A.; Alawak, M.; El-Said Azzazy, H. M.; Bakowsky, U.; Shoeib, T. Thermosensitive Liposomes Encapsulating Nedaplatin and Picoplatin Demonstrate Enhanced Cytotoxicity against Breast Cancer Cells. *ACS Omega* **2022**, *7* (46), 42115−42125.
(13) Sedky, N. K.; Arafa, K. K.; Abdelhady, M. M.; Issa, M. Y.; Abdel-Kader, N. M.; Mahdy, N. K.; Mokhtar, F. A.; Alfaifi, M. Y.; Fahmy, S. A. Nedaplatin/Peganum harmala Alkaloids Co-Loaded Electrospun, Implantable Nanofibers: A Chemopreventive Nano-Delivery System for Treating and Preventing Breast Cancer Recurrence after Tumorectomy. *Pharmaceutics* **2023**, *15* (10), 2367.
(14) Fahmy, S. A.; Ponte, F.; Abd El-Rahman, M. K.; Russo, N.; Sicilia, E.; Shoeib, T. Investigation of the host-guest complexation between 4-sulfocalix [4] arene and nedaplatin for potential use in drug delivery. *Spectrochim. Acta, Part A* **2018**, *193*, 528−536.
(15) Aboeita, N. M.; Fahmy, S. A.; El-Sayed, M. M.; Azzazy, H. M. E.-S.; Shoeib, T. Enhanced anticancer activity of nedaplatin loaded onto copper nanoparticles synthesized using red algae. *Pharmaceutics* **2022**, *14* (2), 418.
(16) El-Shafie, S.; Fahmy, S. A.; Ziko, L.; Elzahed, N.; Shoeib, T.; Kakarougkas, A. Encapsulation of nedaplatin in novel pegylated liposomes increases its cytotoxicity and genotoxicity against a549 and u2os human cancer cells. *Pharmaceutics* **2020**, *12* (9), 863.
(17) Fahmy, S. A.; Ponte, F.; Fawzy, I. M.; Sicilia, E.; Bakowsky, U.; Azzazy, H. M. E.-S. Host-Guest Complexation of Oxaliplatin and Para-Sulfonatocalix [n] Arenes for Potential Use in Cancer Therapy. *Molecules* **2020**, *25* (24), 5926.
(18) Golombek, S. K.; May, J.-N.; Theek, B.; Appold, L.; Drude, N.; Kiessling, F.; Lammers, T. Tumor targeting via EPR: Strategies to enhance patient responses. *Adv. Drug Delivery Rev.* **2018**, *130*, 17−38.
(19) Fahmy, S. A.; Mahdy, N. K.; Al Mulla, H.; ElMeshad, A. N.; Issa, M. Y.; Azzazy, H. M. E.-S. PLGA/PEG nanoparticles loaded with cyclodextrin-Peganum harmala alkaloid complex and ascorbic acid with promising antimicrobial activities. *Pharmaceutics* **2022**, *14* (1), 142.
(20) Silva, M. M.; Calado, R.; Marto, J.; Bettencourt, A.; Almeida, A. J.; Gonçalves, L. Chitosan nanoparticles as a mucoadhesive drug delivery system for ocular administration. *Mar. Drugs* **2017**, *15* (12), 370.
(21) Vasconcelos, D. P.; Fonseca, A. C.; Costa, M.; Amaral, I. F.; Barbosa, M. A.; Águas, A. P.; Barbosa, J. N. Macrophage polarization following chitosan implantation. *Biomaterials* **2013**, *34* (38), 9952−9959.
(22) Almeida, C. R.; Serra, T.; Oliveira, M. I.; Planell, J. A.; Barbosa, M. A.; Navarro, M. Impact of 3-D printed PLA-and chitosan-based scaffolds on human monocyte/macrophage responses: unraveling the effect of 3-D structures on inflammation. *Acta Biomater.* **2014**, *10* (2), 613−622.
(23) Adhikari, H. S.; Yadav, P. N. Anticancer activity of chitosan, chitosan derivatives, and their mechanism of action. *Int. J. Biomater.* **2018**, *2018*, 1−29.
(24) Lima, B. V.; Oliveira, M. J.; Barbosa, M. A.; Goncalves, R. M.; Castro, F. Immunomodulatory potential of chitosan-based materials for cancer therapy: a systematic review of in vitro, in vivo and clinical studies. *Biomater. Sci.* **2021**, *9* (9), 3209−3227.
(25) Peniche, H.; Peniche, C. Chitosan nanoparticles: a contribution to nanomedicine. *Polym. Int.* **2011**, *60* (6), 883−889.
(26) Park, J. H.; Lee, S.; Kim, J.-H.; Park, K.; Kim, K.; Kwon, I. C. Polymeric nanomedicine for cancer therapy. *Prog. Polym. Sci.* **2008**, *33* (1), 113−137.
(27) Fahmy, S. A.; Ponte, F.; Fawzy, I. M.; Sicilia, E.; Azzazy, H. M. E.-S. Betaine host-guest complexation with a calixarene receptor: Enhanced in vitro anticancer effect. *RSC Adv.* **2021**, *11* (40), 24673−24680.
(28) Craig, S. A. Betaine in human nutrition. *Am. J. Clin. Nutr.* **2004**, *80* (3), 539−549.
(29) Zeng, F.; Xu, C.; Liu, Y.; Fan, Y.; Lin, X.; Lu, Y.; Zhang, C.; Chen, Y. Choline and betaine intakes are associated with reduced risk of nasopharyngeal carcinoma in adults: a case-control study. *Br. J. Cancer* **2014**, *110* (3), 808−816.
(30) Fahmy, S. A.; Ramzy, A.; Mandour, A. A.; Nasr, S.; Abdelnaser, A.; Bakowsky, U.; Azzazy, H. M. E.-S. PEGylated chitosan nanoparticles encapsulating ascorbic acid and oxaliplatin exhibit dramatic apoptotic effects against breast cancer cells. *Pharmaceutics* **2022**, *14* (2), 407.
(31) Calvo, P.; Remuñan-López, C.; Vila-Jato, J. L.; Alonso, M. J. Chitosan and chitosan/ethylene oxide-propylene oxide block copolymer nanoparticles as novel carriers for proteins and vaccines. *Pharm. Res.* **1997**, *14*, 1431−1436.
(32) Abdel-Hafez, S. M.; Hathout, R. M.; Sammour, O. A. Tracking the transdermal penetration pathways of optimized curcumin-loaded chitosan nanoparticles via confocal laser scanning microscopy. *Int. J. Biol. Macromol.* **2018**, *108*, 753−764.
(33) Mohammadpour Dounighi, N.; Eskandari, R.; Avadi, M. R.; Zolfagharian, H.; Mir Mohammad Sadeghi, A.; Rezayat, M. Preparation and in vitro characterization of chitosan nanoparticles containing Mesobuthus eupeus scorpion venom as an antigen delivery system. *J. Venomous Anim. Toxins Incl. Trop. Dis.* **2012**, *18*, 44−52.
(34) Batcioglu, K.; Uyumlu, A. B.; Satilmis, B.; Yildirim, B.; Yucel, N.; Demirtas, H.; Onkal, R.; Guzel, R. M.; Djamgoz, M. B. Oxidative Stress in the in vivo DMBA Rat Model of Breast Cancer: Suppression by a Voltage-gated Sodium Channel Inhibitor (RS 100642). *Basic Clin. Pharmacol. Toxicol.* **2012**, *111* (2), 137−141.
(35) Uehara, T.; Watanabe, H.; Itoh, F.; Inoue, S.; Koshida, H.; Nakamura, M.; Yamate, J.; Maruyama, T. Nephrotoxicity of a novel antineoplastic platinum complex, nedaplatin: a comparative study with cisplatin in rats. *Arch. Toxicol.* **2005**, *79*, 451−460.
(36) Matsumoto, M.; Takeda, Y.; Maki, H.; Hojo, K.; Wada, T.; Nishitani, Y.; Maekawa, R.; Yoshioka, T. Preclinical in vivo antitumor efficacy of nedaplatin with gemcitabine against human lung cancer. *Cancer Sci.* **2001**, *92* (1), 51−58.
(37) Fahmy, S. A.; Fawzy, I. M.; Saleh, B. M.; Issa, M. Y.; Bakowsky, U.; Azzazy, H. M. E.-S. Green synthesis of platinum and palladium

https://doi.org/10.1021/acsomega.3c05359
ACS Omega 2023, 8, 41485−41494

nanoparticles using Peganum harmala L. seed alkaloids: Biological and computational studies. *Nanomaterials* **2021**, *11* (4), 965.
(38) Fahmy, S. A.; Azzazy, H. M. E.-S.; Schaefer, J. Liposome photosensitizer formulations for effective cancer photodynamic therapy. *Pharmaceutics* **2021**, *13* (9), 1345.
(39) Azzazy, H. M. E.-S.; Sawy, A. M.; Abdelnaser, A.; Meselhy, M. R.; Shoeib, T.; Fahmy, S. A. Peganum harmala Alkaloids and Tannic Acid Encapsulated in PAMAM Dendrimers: Improved Anticancer Activities as Compared to Doxorubicin. *ACS Appl. Polym. Mater.* **2022**, *4* (10), 7228−7239.
(40) Shi, L.; Zhang, J.; Zhao, M.; Tang, S.; Cheng, X.; Zhang, W.; Li, W.; Liu, X.; Peng, H.; Wang, Q. Effects of polyethylene glycol on the surface of nanoparticles for targeted drug delivery. *Nanoscale* **2021**, *13* (24), 10748−10764.
(41) Zhang, X.; Teng, D.; Wu, Z.; Wang, X.; Wang, Z.; Yu, D.; Li, C. PEG-grafted chitosan nanoparticles as an injectable carrier for sustained protein release. *J. Mater. Sci.: Mater. Med.* **2008**, *19*, 3525−3533.
(42) Chen, Y.; Wu, D.; Zhong, W.; Kuang, S.; Luo, Q.; Song, L.; He, L.; Feng, X.; Tao, X. Evaluation of the PEG density in the PEGylated chitosan nanoparticles as a drug carrier for curcumin and mitoxantrone. *Nanomaterials* **2018**, *8* (7), 486.
(43) Viertorinne, M.; Valkonen, J.; Pitkänen, I.; Mathlouthi, M.; Nurmi, J. Crystal and molecular structure of anhydrous betaine, (CH3)3NCH2CO2. *J. Mol. Struct.* **1999**, *477* (1−3), 23−29.
(44) Shimada, M.; Itamochi, H.; Kigawa, J. Nedaplatin: a cisplatin derivative in cancer chemotherapy. *Cancer Manage. Res.* **2013**, *5*, 67−76.
(45) Torres, M.; Khan, S.; Duplanty, M.; Lozano, H. C.; Morris, T. J.; Nguyen, T.; Rostovtsev, Y. V.; DeYonker, N. J.; Mirsaleh-Kohan, N. Raman and infrared studies of platinum-based drugs: cisplatin, carboplatin, oxaliplatin, nedaplatin, and heptaplatin. *J. Phys. Chem. A* **2018**, *122* (34), 6934−6952.
(46) Azzazy, H. M. E.-S.; Fahmy, S. A.; Mahdy, N. K.; Meselhy, M. R.; Bakowsky, U. Chitosan-coated PLGA nanoparticles loaded with Peganum harmala alkaloids with promising antibacterial and wound healing activities. *Nanomaterials* **2021**, *11* (9), 2438.
(47) Boonsongrit, Y.; Mueller, B. W.; Mitrevej, A. Characterization of drug-chitosan interaction by 1H NMR, FTIR and isothermal titration calorimetry. *Eur. J. Pharm. Biopharm.* **2008**, *69* (1), 388−395.
(48) Sarwar, M. S.; Ghaffar, A.; Islam, A.; Yasmin, F.; Oluz, Z.; Tuncel, E.; Duran, H.; Qaiser, A. A. Controlled drug release behavior of metformin hydrogen chloride from biodegradable films based on chitosan/poly (ethylene glycol) methyl ether blend. *Arabian J. Chem.* **2020**, *13* (1), 393−403.
(49) Mariadoss, A. V. A.; Vinayagam, R.; Senthilkumar, V.; Paulpandi, M.; Murugan, K.; Xu, B.; Km, G.; Kotakadi, V. S.; David, E. Phloretin loaded chitosan nanoparticles augments the pH-dependent mitochondrial-mediated intrinsic apoptosis in human oral cancer cells. *Int. J. Biol. Macromol.* **2019**, *130*, 997−1008.
(50) Nallamuthu, I.; Devi, A.; Khanum, F. Chlorogenic acid loaded chitosan nanoparticles with sustained release property, retained antioxidant activity and enhanced bioavailability. *Asian J. Pharm. Sci.* **2015**, *10* (3), 203−211.
(51) Meng, J.; Sturgis, T. F.; Youan, B.-B. C. Engineering tenofovir loaded chitosan nanoparticles to maximize microbicide mucoadhesion. *Eur. J. Pharm. Sci.* **2011**, *44* (1−2), 57−67.
(52) Ulu, A.; Sezer, S. K.; Yüksel, Ş.; Koç, A.; Ateş, B. Preparation, Controlled Drug Release, and Cell Viability Evaluation of Tenofovir Alafenamide-Loaded Chitosan Nanoparticles. *Starch* **2021**, 2100144.
(53) Zhang, T.; Sturgis, T. F.; Youan, B.-B. C. pH-responsive nanoparticles releasing tenofovir intended for the prevention of HIV transmission. *Eur. J. Pharm. Biopharm.* **2011**, *79* (3), 526−536.
(54) Malhotra, M.; Lane, C.; Tomaro-Duchesneau, C.; Saha, S.; Prakash, S. A novel method for synthesizing PEGylated chitosan nanoparticles: strategy, preparation, and in vitro analysis. *Int. J. Nanomed.* **2011**, *6*, 485−494.
(55) Lin, W.; Lee, H.; Wang, D. The influence of plasticizers on the release of theophylline from microporous-controlled tablets. *J. Controlled Release* **2004**, *99* (3), 415−421.
(56) Browning, R. J.; Reardon, P. J. T.; Parhizkar, M.; Pedley, R. B.; Edirisinghe, M.; Knowles, J. C.; Stride, E. Drug delivery strategies for platinum-based chemotherapy. *ACS Nano* **2017**, *11* (9), 8560−8578.
(57) Jia, C.; Zhong, Y.; Zhang, X.; Liao, X.; Li, Y.; Yang, B.; Gao, C. Host-guest inclusion systems of nedaplatin with cucurbit [7] uril for improved in vitro antitumour activity. *J. Inclusion Phenom. Macrocyclic Chem.* **2020**, *97*, 99−107.
(58) Wang, M.; Thanou, M. Targeting nanoparticles to cancer. *Pharmacol. Res.* **2010**, *62* (2), 90−99.
(59) Lu, B.; Lv, X.; Le, Y. Chitosan-modified PLGA nanoparticles for control-released drug delivery. *Polymers* **2019**, *11* (2), 304.
(60) Huang, S.-J.; Wang, T.-H.; Chou, Y.-H.; Wang, H.-M. D.; Hsu, T.-C.; Yow, J.-L.; Tzang, B.-S.; Chiang, W.-H. Hybrid PEGylated chitosan/PLGA nanoparticles designed as pH-responsive vehicles to promote intracellular drug delivery and cancer chemotherapy. *Int. J. Biol. Macromol.* **2022**, *210*, 565−578.

https://doi.org/10.1021/acsomega.3c05359
ACS Omega 2023, 8, 41485−41494